A Differential Polarized Phase Fluorometric Study of the Effects of High Hydrostatic Pressure upon the Fluidity of Cellular Membranes[†]

Parkson L.-G. Chong and Andrew R. Cossins[*,‡]

Appendix: Correction of Experimental Tangent in Differential Polarized Phase Fluorometry When Emission Traverses the Birefringent Windows of a High-Pressure Bomb

Gregorio Weber

ABSTRACT: The effects of high hydrostatic pressure (up to 2 kbar) upon the fluidity and order of the synaptic and myelin membrane fractions of goldfish brain have been studied by using steady-state and differential polarized phase fluorometry. Probe motion provided a measure of membrane order (r_∞) and probe rotational rate (R). Membrane order became progressively greater as pressure was increased up to approximately 2 kbar. This effect was similar over the temperature range 5.6–34.3 °C. An increase in pressure of 1 kbar had an effect on membrane order that was equivalent to a 13–19 °C reduction in temperature. Membrane order was essentially identical during pressurization and depressurization. At 5.6 °C, pressurization caused a large increase in R, and similar, though less dramatic, anomalies occurred at higher temperatures. It is suggested that this is due to the segregation of probe molecules in highly ordered membranes, which leads either to excitation transfer between 1,6-diphenyl-1,3,5-hexatriene (DPH) molecules or to changes in the rotational motion of DPH from "sticking" to "slipping".

H ydrostatic pressure is a thermodynamic variable with potentially disruptive influences on the normal physiological and biochemical activities of living organisms. Although the fundamental physicochemical bases of pressure-induced effects are well established, the scale of these effects, or their importance at the pressures to which living organisms may be exposed, is comparatively poorly defined. For biological membranes, this is mainly because biophysical techniques for the analysis of membrane dynamic structure (fluidity) and functional properties at high pressure are poorly developed.

Studies on the phase transitions of smectic mesophases (liposomes) of defined phospholipids are a popular means by which to understand the behavior of membrane systems in general. Isothermal phase transitions can be induced in such systems by increased pressure; thus, at 1 kbar the transition temperature of dipalmitoyllecithin is increased by 17–30 °C [reviewed in Wann & MacDonald (1980); see also P. L.-G. Chong and G. Weber (unpublished results)]. Phase transitions in biological membranes are usually less cooperative and more difficult to detect than in artificial membranes. Nevertheless, Gause et al. (1974) have detected a putative lipid phase transition in rabbit macrophage membranes with ESR[1] spectroscopy and also found a dT/dP of 27 K/1000 atm.

Measurements of membrane fluidity, rather than phase state, are less frequent since they require the use of more sophisticated spectroscopic techniques. Chin et al. (1976), using spin-labeled phosphatidylcholine, showed a linear increase of an empirical order parameter of phospholipid liposomes with increased pressure. On the other hand, Finch et al. (1979) measured the fluidity of erythrocyte membranes and found that the hydrophobic interior was hardly affected by pressures up to 100 atm, whilst the hydrophilic region of the bilayer became less fluid.

A popular technique for the estimation of membrane fluidity is fluorescence polarization of the rod-shaped fluorophore 1,6-diphenyl-1,3,5-hexatriene (DPH). Until recently, polarization measurements made under steady-state excitation have been interpreted on the basis of the Perrin equation, which assumed unhindered, isotropic rotations of the fluorophore (Shinitzky et al., 1971; Shinitzky & Barenholz, 1978). This provided a measure of the rate of probe rotation that was thought to reflect the dynamic motion of the membrane interior. Recent time-resolved anisotropy measurements have revealed that probe rotation is severely restricted by the anisotropic nature of its hydrocarbon environment (Kawato et al., 1977; Chen et al., 1977; Lakowicz et al., 1979) so that the probe undergoes wobbling motion within a restricted cone (Kinosita et al., 1977). Indeed, the steady-state anisotropies usually measured in biological membranes are determined principally by the degree to which probe rotations are restricted (i.e., a measure of order) rather than by its rotational rate (a dynamic measure).

The main problem with the use of this technique at high pressures is the birefringency of the quartz windows of the pressurized vessel chambers as they suffer deformation and mechanical stress (photoelastic effects). Paladini & Weber (1981) have recently described a correcting procedure for the photoelastic effects and have constructed a pressure vessel to enable the measurement of polarization at pressures up to 2 kbar. In this study, we have used this apparatus to measure the interacting effects of pressure and temperature upon the fluidity or membrane order of brain membrane fractions of goldfish.

The principal objective of the study was to determine the magnitude of pressure-induced changes in membrane structure

[1] Abbreviations: ESR, electron spin resonance; DPH, 1,6-diphenyl-1,3,5-hexatriene.

and to provide an estimate of the consequences for living membranes subject to high hydrostatic pressure. In order to provide measures of membrane order as well as the motional rates of the membrane interior, we have combined steady-state polarization measurements with differential polarized phase measurements as described by Weber (1978) and Lakowicz et al. (1979).

Materials and Methods

Animals. Goldfish (8–10-cm length) were obtained from a commercial source and maintained for at least 3 weeks at 5 °C with a 12 h light/12 h dark photoperiod.

Preparation of Membrane Fractions. Brain synaptic and myelin membrane fractions were prepared exactly as described by Cossins & Prosser (1982). Membrane preparations were stored at 0 °C until required.

Fluorescence Polarization. Emission polarization was measured in a photon-counting, T-format fluorometer similar to that described by Jameson et al. (1980) except that the normal cuvette chamber was replaced by the pressure vessel described in detail by Paladini & Weber (1981). The excitation beam (358 nm) was filtered by a 4-mm Corning CS7-54 broad band-pass filter and the emission viewed through Corning CS3-73 and 2-mm thickness of 2 M $NaNO_2$. The pressure-induced birefringency of the quartz windows of the pressure vessel was corrected as described by Paladini & Weber (1981). The membrane suspension (OD_{500} = 0.1) was labeled by adding 2 µL of 2 mM DPH in tetrahydrofuran with vigorous stirring, as described by Cossins (1977). The sample was placed in a round quartz cuvette and sealed from the hydrostatic fluid (ethanol) by a collapsible polyethylene cap. In order to correct for light-scattering artifacts, we made identical measurements on unlabeled membrane suspensions, and these values were subtracted from the fluorescence intensities. In any event, scattered light accounted for only 0.5–1.0% of total emission of DPH-labeled membrane. The standard deviation of the polarization values is approximately ±0.001.

The temperature of the pressure vessel was controlled to ±0.2 °C by a Neslab thermostated circulator. It was measured to ±0.1 °C with a thermocouple inserted into a hole close to the pressurized cuvette. The sample was equilibrated for at least 5 min after each pressure change before measurements were started.

Fluorescence Lifetime. Fluorescence lifetime was measured by using the cross-correlation phase fluorometer described by Spencer & Weber (1969), but with improved electronics (SLM Instruments, Urbana, IL). Modulation frequency was 18 MHz, and the excitation wavelength and excitation and emission filters were as described for the polarization measurements. A suspension of glycogen in millipore water (10^8 Ω cm^{-2}) was used to provide a scattered reference signal of approximately equal intensity to the DPH-labeled suspension of membranes. When this was required, light was reflected from the excitation beam with a quartz plate through an alternate pathway of exactly equal length to the pathway used during normal measurements.

Some "color" effect was noticed with the photomultipliers (Phillips 1023) and was corrected by using the procedure described by Jameson & Weber (1981). Fluorescence lifetime was measured by phase delay and by demodulation techniques (Spencer & Weber, 1969). The values obtained were the average of several-hundred measurements, typically with a standard deviation of 20–50 ps. The average of the lifetime determined by phase and modulation methods was used in subsequent calculations.
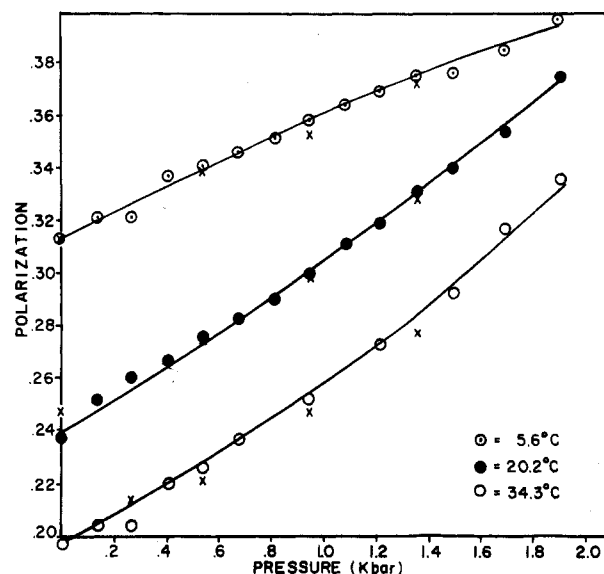

FIGURE 1: Effects of pressure upon steady-state polarization for DPH in synaptic membrane fraction of goldfish brain. All values were corrected for light-scattering artifacts and for pressure-induced birefringency of pressure vessel windows. *X* values, used in Figures 1–5, were obtained during depressurization.

Differential Lifetime. The differential lifetime was measured as described by Cossins et al. (1980) except that the normal cuvette chamber was replaced by the pressure vessel. Modulation frequency was 18 MHz, and the excitation wavelength and filters were as described for the polarization measurements. The effects of the pressure-induced birefringency of the quartz windows of the pressure vessel upon the differential lifetime were corrected as described in the Appendix. The standard deviation of the differential lifetime values is approximately ±0.025 ns.

The lower limiting anisotropy (r_∞), the average amplitude of rotation (θ), and the rotational rate (R) were calculated from the measured values of p, τ, and $\Delta\tau$ with the theory developed by Weber (1978) and extended by Lakowicz et al. (1979). Briefly, the lower limiting anisotropy (r_∞) is the lowest value of anisotropy attainable at times that are long compared to the fluorescence lifetime. The average amplitude of rotation (θ) is the average amplitude of the angular distribution of the probe about an axis normal to the membrane plane at times that are long compared with the fluorescence lifetime. Both r_∞ and θ reflect the degree of constraint imposed upon the motion of the probe by its neighboring molecules. The rotational diffusion coefficient, R, is an aggregate term that reflects the average rate of rotation of the probe within the highly anisotropic lipid environment. The limiting anisotropy (r_0) was determined in the polarization fluorometer with the pressure vessel in position and was found to be 0.38. D_w was calculated as described by Kinosita et al. (1977) with values of θ that were estimated from their Figure 3b.

Results

The effects of pressure upon the steady-state polarization of DPH in synaptic membranes of goldfish are illustrated in Figure 1. At each temperature, there was a progressive increase in polarization with increased pressure. The slope of the graphs was somewhat less at 5.6 °C than at higher temperatures so that at higher pressures the values of polarization at 5.6 °C and 20 °C approach each other. Polarization measured during pressurization and depressurization were almost identical.

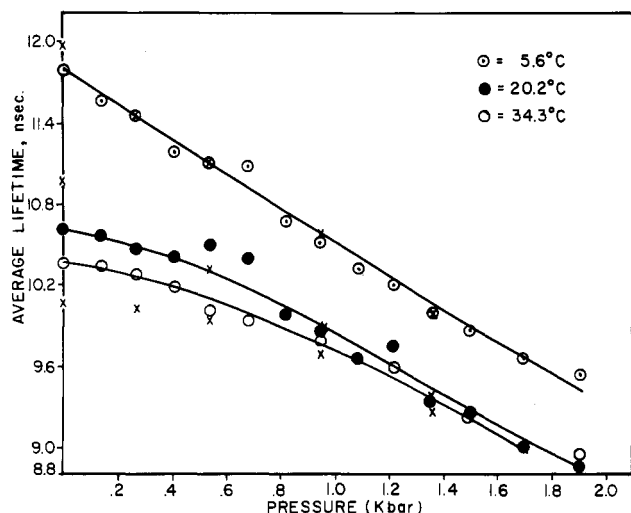In Figure 2, the fluorescent lifetime of DPH (τ_{av}) is plotted

FIGURE 2: Effects of pressure upon fluorescence lifetimes of DPH in synaptic membrane fraction of goldfish brain. Lifetimes were the average of the lifetime measured by phase delay and demodulation techniques. The lifetime by phase delay was corrected for color effect according to the method of Jameson & Weber (1981).
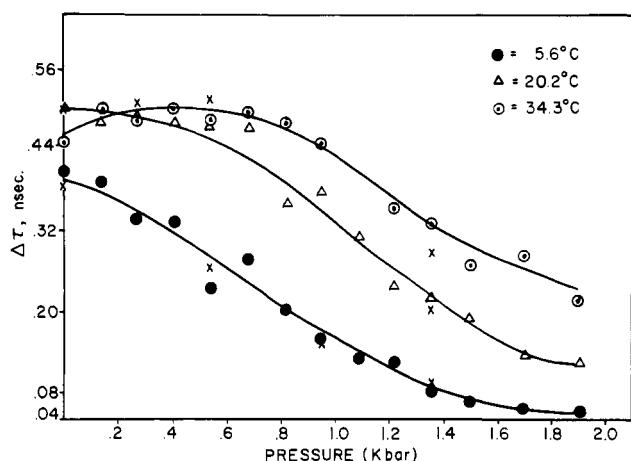

FIGURE 3: Effects of pressure upon differential lifetime of DPH in synaptic membrane fraction of goldfish brain. $\Delta\tau$ values were corrected for the pressure-induced birefringency of the quartz windows of the pressure vessel as described in the Appendix.

FIGURE 4: Effects of pressure upon lower limiting anisotropy, r_∞ (A), and average angular amplitude, θ (B), of DPH in synaptic membrane fraction of goldfish brain. Values were calculated as described by Weber (1978) and Lakowicz et al. (1979).

against pressure. Again, there was a nearly linear effect of pressure upon lifetime with similar slopes at each temperature. Values obtained during pressurization and depressurization were almost identical.

In Figure 3 the differential lifetime is plotted against pressure. The maximal values of $\Delta\tau$ obtained at atmospheric pressure (approximately 0.5 ns) were considerably less than the value calculated for isotropic, unhindered rotations (Cossins et al., 1980; Cossins & Prosser, 1982). This indicates that probe motion was indeed hindered (Weber, 1978) and that the Perrin equation is inappropriate in this case. The curves resembled the smooth bell-shaped curves obtained when temperature alone was varied (Lakowicz et al., 1979; Cossins et al., 1980) and are what one would expect from the theoretical relationship between $2R\tau$ and $\Delta\tau$ (Weber, 1978). Thus, pressurization at 5.6 °C results in a smooth, progressive decline in $\Delta\tau$ whereas at higher temperatures the curves pass through a maximum of approximately 0.5 ns. The effect of pressure upon $\Delta\tau$ was entirely reversible.

The lower limiting anisotropy (r_∞) and rotational rate (R) were calculated from the measured values of polarization, τ, and $\Delta\tau$ according to the theory of Weber (1978). The lower limiting anisotropy increased progressively with pressure. At
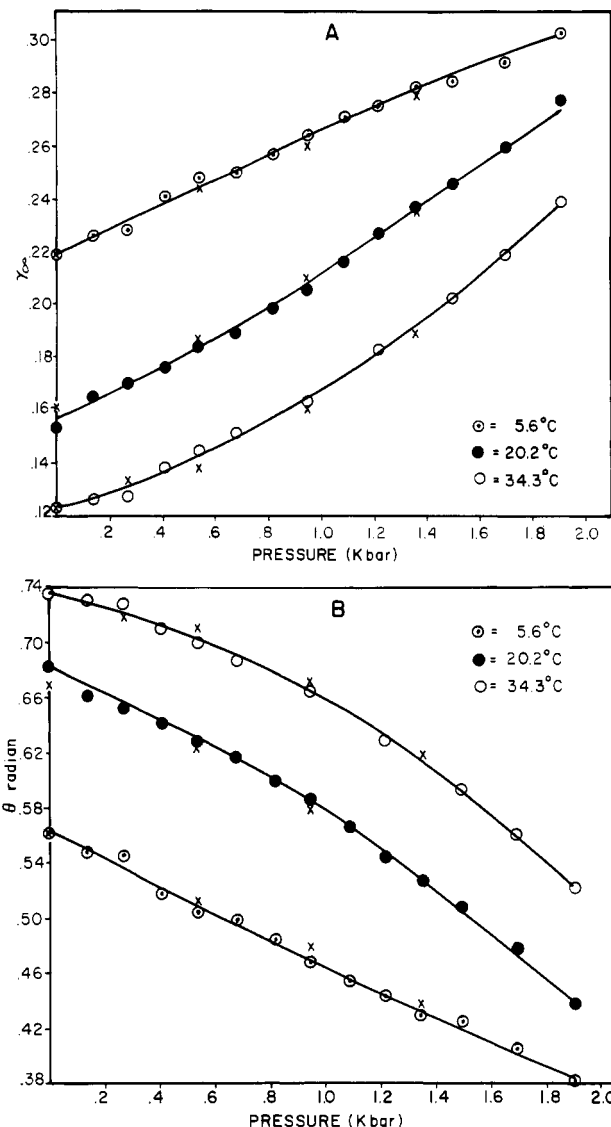
5.6 °C this relationship was linear (Figure 4A), but at higher temperatures the graphs were curvilinear such that at high pressures the values at 5.6 and 20.2 °C became more similar. Figure 4B illustrates the effect of pressure on the average angular amplitude of rotation (θ). At 5.6 °C, $\theta = 32°$ at atmospheric pressure and 22° at 1.9 kbar. The reduction in θ was equally dramatic at 20.2 and 34.4 °C.

The effect of pressure on R was complex (Figure 5). At atmospheric pressure, R increased with temperature such as one would expect (Cossins & Prosser, 1982). Increased pressure at 5.6 °C resulted in an increase in R, which is large when compared to the effects of temperature at atmospheric pressure. At higher temperatures, the curves were biphasic with a slight decrease at pressures up to 0.6–0.8 kbar and a slight increase at higher temperatures.

The equivalence between the effects of temperature and pressure upon membrane fluidity was determined from Figures 1 and 4 by measuring the shift of respective graphs along the pressure axis for an approximate 15 °C increase in temperature. Values were calculated as degrees Celsius per kilobar and are presented in Table I for the temperature ranges 5–20 and 20–35 °C.
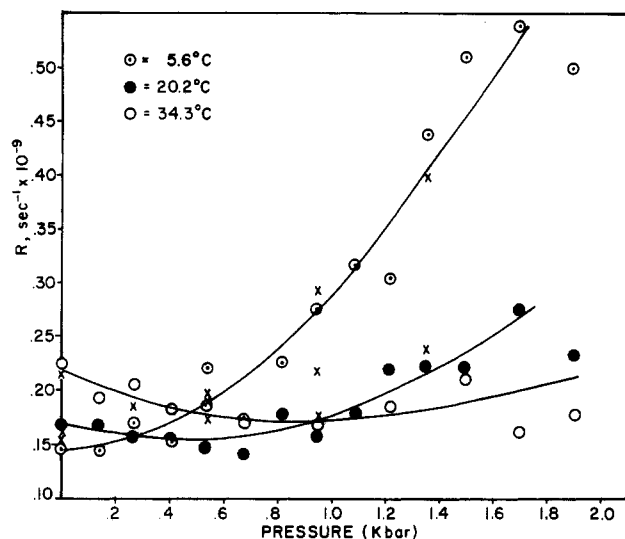
FIGURE 5: Effects of pressure upon rotational rate (R) of DPH in synaptic membrane fraction of goldfish. Other details are as in the legend to Figure 4.

Table I: Temperature–Pressure Equivalence for Polarization and r_∞ for DPH in Brain Synaptic and Myelin Membrane Fractions of Goldfish

membrane fraction	parameter	dT/dP (°C kbar^{-1})^a	
		5–20 °C	20–35 °C
synaptic	polarization	13.0	18.8
	r_∞	13.2	17.0
myelin	polarization	13.9	18.6

^{a} Values were obtained from Figures 1 (polarization) and 4 (r_∞) by calculating the difference in pressure for identical values of polarization or r_∞ at the two temperatures. The temperature difference was divided by the pressure difference.

Discussion

The differential polarized phase measurements show that the depolarizing motion of DPH in both synaptic and myelin membranes is hindered, in agreement with previous work (Cossins et al., 1980; Cossins & Prosser, 1982). The data, therefore, have been treated according to the "wobbling-in-cone" model of Kinosita et al. (1977) by the observation of differential phase fluorometry. This analysis gives two measures of probe motion, the lower limiting anisotropy (r_∞) and the rotational rate (R).

The measures of membrane static order (polarization, r_∞, and θ) indicate that increased hydrostatic pressure has a progressive ordering effect upon the environment of the probe. This is presumably due to the reduction in volume of the bilayer under pressure and a reduction in the cross-sectional area per phospholipid molecule. The bulk compressibility of dipalmitoyllecithin liposomes in the liquid-crystalline state has been estimated by dilatometry as approximately 0.1 mL mol^{-1} atm^{-1} (Liu & Kay, 1977). Stomatoff et al. (1978) have demonstrated that the bilayer thickness actually increases with pressure so that the lateral compressibility of the bilayer plays the dominant role in pressure-mediated effects.

The ordering effects of hydrostatic pressure are appreciable; thus, a pressure of 1 kbar reduces membrane fluidity by approximately the same amount as a 13–19 °C reduction in temperature. Another means of demonstrating the temperature-to-pressure equivalency is by plotting the steady-state anisotropy, r_s, against the lower limiting anisotropy, r_∞, to see whether the relation produced by varying pressure is equivalent to the one produced by temperature variations. Figure 6 shows
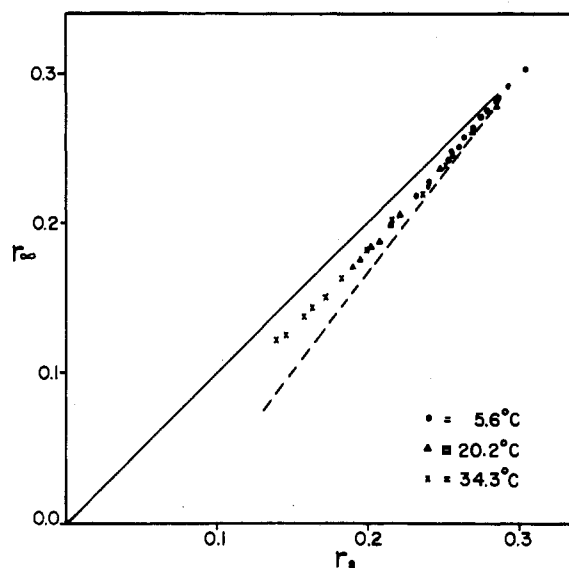

FIGURE 6: Lower limiting anisotropy (r_∞) of DPH as a function of steady-state anisotropy (r_s) for synaptic membrane fraction of goldfish. Data [(×) 34.3 °C; (▲) 20.2 °C; (●) 5.6 °C] from this study were compared with the data (−−) using liposomes (van Blitterswijk et al., 1981). (—) The case when $r_\infty = r_s$.

that the lines for three temperatures are contiguous; that is, temperature and pressure are fully interchangeable in terms of their effects on static order. The slope of our line is similar to those found for cholesterol-containing liposomes but slightly above that observed for cholesterol-free liposomes by van Blitterswijk et al. (1981). This equivalency between temperature and pressure is similar to the range (15–27 °C/kbar) found by a number of workers for the increase in transition temperature (Wann & MacDonald, 1980; P. L.-G. Chong and G. Weber, unpublished results) and the increase in the temperature of the Arrhenius discontinuity of the activity of several membrane-bound enzymes caused by high pressure (Ceuterick et al., 1978; MacDonald & MacNaughton, 1982; Ceuterick et al., 1979; de Smedt et al., 1979). By comparison, the effects of pressure upon structural transitions of aqueous proteins and DNA are very small [1–6 °C/kbar; reviewed in Heremans (1980)]. Phospholipid bilayers and biological membranes have appreciable compressibilities. This is made possible by the expanded nature of the hydrocarbon chains in liquid-crystalline phase that is typical of membranes of higher organisms at physiological temperatures. Membranes in the ordered phase are considerably less compressible (Liu & Kay, 1977).

There appears to be no obvious evidence of pressure-induced phase transitions in goldfish membranes such as those observed in phospholipid liposomes by P. L.-G. Chong and G. Weber (unpublished results), even at the very high and nonphysiological pressures used in this study. Another important observation of the experiments described here was the near complete reversibility of pressure-induced effects on membrane order. The values of polarization, τ_{av}, and $\Delta\tau$ were essentially the same during pressurization up to 2 kbar and subsequent depressurization.

The increase in R and the wobbling diffusion constant, D_w, (Figure 7) at 5.6 °C with increasing hydrostatic pressure appears to contradict the ordering effects of pressure described previously. It is certainly possible that the progressive constraint imposed upon the rotational amplitude of DPH may lead to an increase in the rate of motion within this restricted cone. On the other hand, this increase was far in excess of that produced at atmospheric pressure by a 30 °C rise in temperature, which suggests some anomaly in the behavior
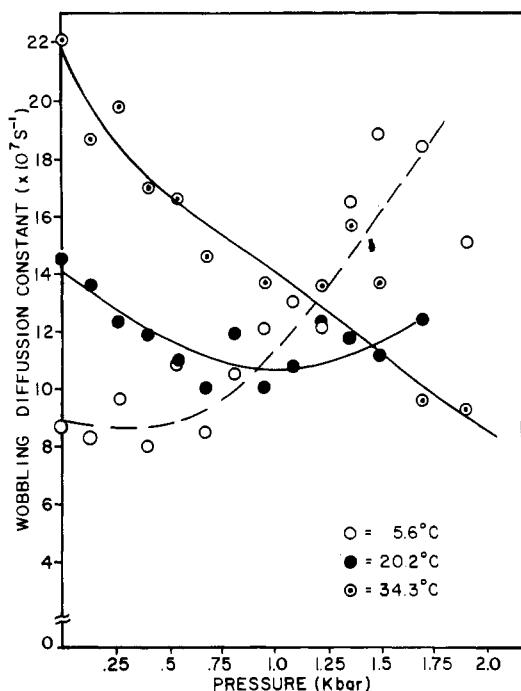
FIGURE 7: Effects of pressure upon wobbling diffusion constant (D_w) of DPH in synaptic membrane fraction of goldfish. Values were calculated according to the method of Kinosita et al. (1977).

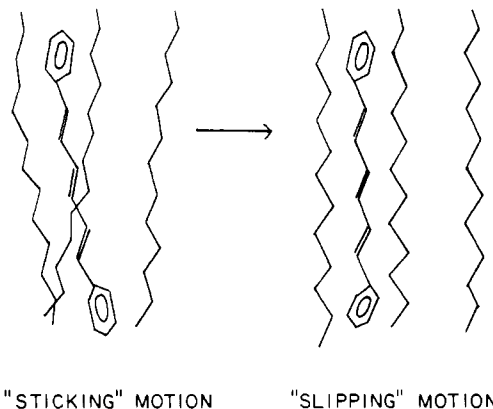"STICKING" MOTION   "SLIPPING" MOTION

FIGURE 8: Rotational motion of DPH changes from sticking to slipping when the lipid bilayer becomes more ordered, at low temperature and high pressure.

of DPH in these membranes under pressure.

Several alternative explanations may account for this effect. One possibility is that at pressures in excess of 1 kbar, the hydrogen-bonding structure of aqueous media becomes attenuated (de Fries & Jonas, 1977). This would reduce the thermodynamic driving force for the formation of bilayers and for the sequestration of DPH molecules within the hydrophobic domain of bilayers. As the pressure is raised, the probe may come to occupy a qualitatively different site, one in which rotational motion is less hindered. This should become evident not only as an increase in R but also as a dramatic reduction in the lower limiting anisotropy, which is certainly not the case in this instance.

Alternatively, the combined ordering effects of low temperature and high pressure may result in the segregation of probe molecules into a localized domain of lipid molecules that may lead to excitation transfer. This would increase the apparent rotational rate, but since the depolarizing rotations of all DPH molecules would be equally hindered, there should be no dramatic change in r_∞ or θ above that produced by the pressure change. This prediction is in agreement with the results presented here.

The anomaly in R or D_w with increasing pressure could also be explained by changes in the rotational characteristics of the probe. At high temperature and low pressure, the lipid system is less ordered, and the DPH molecules may become entangled with nearby hydrocarbon chains so that the rotation of DPH is actually a "sticking" motion (Hu & Zwanzig, 1974) (Figure 8). On the other hand, at low temperature and high pressure, the lipid bilayer becomes more ordered. The probe may be progressively aligned by the more ordered hydrocarbon chains so that its rotation may result more from "slipping" motions (Hu & Zwanzig, 1974) (Figure 8) rather than from "sticking" motions. The sticking type of rotational motion results in relaxation times about 5–10 times larger than those of the slipping motion, as shown by Hu & Zwanzig (1974). It is interesting to note that the effect of low temperature and high pressure on the wobbling action of DPH in this biological membrane preparation is similar to the effect of low temperature on artificial membranes (Kawato et al., 1977). Similarly, Kawato et al. (1978) and Kinosita et al. (1981) have found that the incorporation of cholesterol and protein, respectively, into artificial bilayers accelerated the wobbling motion of DPH although the cone angle was comparatively unaffected. These authors attribute this effect to the mismatch of membrane components, allowing more independent motion of the probe than would occur in an undisturbed bilayer.

The various interpretations presented here for the anomalous rotational behavior of DPH in highly ordered membranes are amongst the simplest that can be advanced. In the event that DPH binds nonspecifically to different sites within the bilayer, to hydrophobic pockets within proteins (Mêly-Goubert & Freedman, 1980), or to the so-called "boundary layer" of lipids that may surround intrinsic proteins (Kinosita et al., 1981), then it is certainly possible that low temperature and high pressure may combine to cause a shift in the distribution of DPH between these sites. At present, techniques are not available to distinguish between shifts in DPH distribution and changes in the rotational characteristics of a predominant population of fluorophores, and it is acknowledged that both effects may be important to greater or lesser extents.

The results discussed above indicate that pressure does two things: it progressively orders the lipid bilayer packing, but at low temperatures it probably induces a change in the rotational mode. However, it is clear that the range of hydrostatic pressures that exist in the oceans may have very significant effects upon cell membranes in general. At a depth of 4000 m (approximately 400 atm), the ordering effect is equivalent to that produced by a 5–8 °C reduction in temperature. At 10000 m (968 atm), which is approximately the greatest hydrostatic pressure experienced by living organisms, the corresponding value is 10–19 °C. At both depths, the environmental temperature is approximately 3–4 °C. The effects of low temperatures and high pressure summate so that the equivalent temperature for a surface-dwelling organism is in the range −7 to −16 °C, which is certainly the environment with the lowest enthalpic content within which organisms are active for their entire life cycles. There is thus good reason to expect that animals in these environments would display adaptations at the cellular and molecular levels of organization that enhance their performance under these conditions, similar to those that occur in fish endemic to polar regions (Cossins & Prosser, 1978). However, the anomaly observed in the rotational rate of DPH at low temperature and high pressure may ameliorate the probable consequences of life at high pressure upon membrane function, so that a conventional
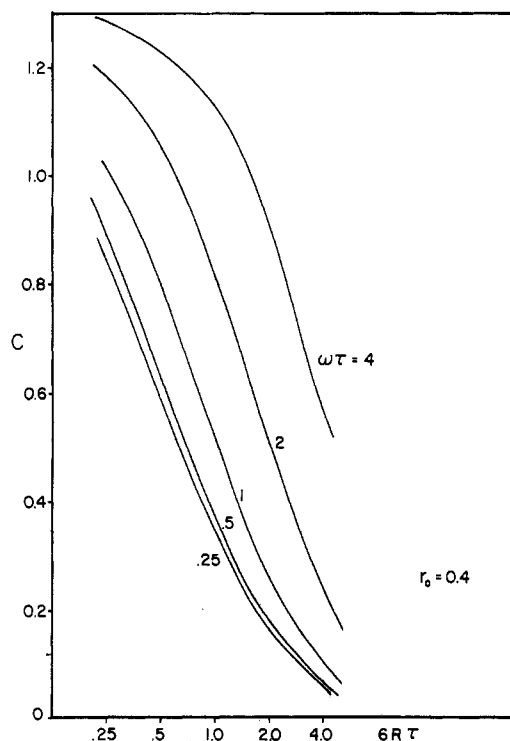
FIGURE 9: Value of C for a single rotation rate (spherical symmetry) as a function of the parameters $\omega\tau$ (circular frequency times lifetime) and $6R\tau$ (6 times rotational rate times lifetime) when the limiting anisotropy, r_0, is 0.4. P and Q values are from eq 17 of Weber (1977).

homeoviscous adaptation of deep-sea organisms compared to surface-dwelling organisms may not be observed.

Acknowledgments

We are grateful to Professor Gregorio Weber for providing the correction procedure, as shown in the Appendix, for the photoelastic effects produced in the differential lifetime measurements, and for use of the instruments in his laboratory. We also thank Dr. R. Dale for helpful discussions and Robert Macgregor for computer assistance.

References

Ceuterick, F., Peeters, J., Heremans, K., de Smedt, H., & Olbrechts, H. (1978) Eur. J. Biochem. 87, 401–407.

Ceuterick, F., Goethals, A. M., Paulssen, N., Wuytack, F., de Smedt, H., & Heremans, K. (1979) Arch. Int. Physiol. Biochim. 87, 1012–1013.

Chen, L. A., Dale, R. E., Roth, S., & Brand, L. (1977) J. Biol. Chem. 252, 2163–2169.

Chin, J. H., Trudell, J. R., & Cohen, E. N. (1976) Life Sci. 18, 489–498.

Cossins, A. R. (1977) Biochim. Biophys. Acta 470, 395–411.

Cossins, A. R., & Prosser, C. L. (1978) Proc. Natl. Acad. Sci. U.S.A. 75, 2040–2043.

Cossins, A. R., & Prosser, C. L. (1982) Biochim. Biophys. Acta 687, 303–309.

Cossins, A. R., Kent, J., & Prosser, C. L. (1980) Biochim. Biophys. Acta 599, 341–358.

de Fries, T., & Jonas, J. (1977) J. Chem. Phys. 66, 896–901.

de Smedt, H., Borghgraef, R., Ceuterick, F., & Heremans, K. (1979) Biochim. Biophys. Acta 556, 479–489.

Finch, E. D., Zwakman, D. S., & Kiesow, L. A. (1979) Undersea Biomed. Res. 6, 41.

Gause, E. M., Menoez, V. M., & Rowlands, J. R. (1974) Spectrosc. Lett. 7, 477–490.

Heremans, K. (1980) in Animals and Environmental Fitness (Gilles, R., Ed.) Vol. 1, pp 427–440, Pergamon Press, Oxford.

Hu, C.-M., & Zwanzig, R. (1974) J. Chem. Phys. 60, 4354–4357.

Jameson, D. M., & Weber, G. (1981) J. Phys. Chem. 85, 953–958.

Jameson, D. M., Weber, G., Spencer, R. D., & Mitchell, G. (1980) Rev. Sci. Instrum. 49, 510–514.

Kawato, S., Kinosita, K., Jr., & Ikegami, A. (1977) Biochemistry 16, 2319–2324.

Kawato, S., Kinosita, K., Jr., & Ikegami, A. (1978) Biochemistry 17, 5026–5031.

Kinosita, K., Kawato, S., & Ikegami, A. (1977) Biophys. J. 20, 289–305.

Kinosita, K., Jr., Kawato, S., Ikegami, A., Yosbede, S., & Orii, Y. (1981) Biochim. Biophys. Acta 647, 7–17.

Lakowicz, J. R., Prendergast, F. G., & Hogan, D. (1979) Biochemistry 18, 508–519.

Liu, N.-I., & Kay, R. L. (1977) Biochemistry 16, 3484–3486.

MacDonald, A. G., & MacNaughton, W. (1982) Comp. Biochem. Physiol. A 72A (2), 405–414.

Mély-Goubert, B., & Freedman, M. H. (1980) Biochim. Biophys. Acta 601, 315–327.

Paladini, A. A., & Weber, G. (1981) Rev. Sci. Instrum. 52 (3), 419–427.

Shinitzky, M., & Barenholz, Y. (1978) Biochim. Biophys. Acta 515, 367–394.

Shinitzky, M., Dianoux, A.-C., Gitler, C., & Weber, G. (1971) Biochemistry 10, 2106–2113.

Spencer, R., & Weber, G. (1969) Ann N.Y. Acad. Sci. 158, 361–376.

Stomatoff, J., Guillon, D., Powers, L., Cladis, P., & Aadsen, D. (1978) Biochem. Biophys. Res. Commun. 85, 724–728.

van Blitterswijk, W. J., van Hoeven, R. P., & van der Meer, B. W. (1981) Biochim. Biophys. Acta 664, 323–332.

Wann, K. T., & MacDonald, A. G. (1980) Comp. Biochem. Physiol. A 66A, 1–12.

Weber, G. (1977) J. Chem. Phys. 66, 4081–4091.

Weber, G. (1978) Acta Phys. Pol. A A54, 859–865.

Appendix: Correction of Experimental Tangent in Differential Polarized Phase Fluorometry When Emission Traverses the Birefringent Windows of a High-Pressure Bomb

Because of the photoelastic effect, the windows subjected to a unilateral pressure become birefringent, and a fraction α of the light incident upon the window emerges polarized in a plane normal to that of the incident ray. It will be assumed that the scrambling coefficient, α, is independent of the azimuth of the incident polarization as this has been justified, for the range of pressures up to 2 kbar by measurements of Paladini (1980). We follow below the notation of Weber (1977) according to which

$$Q_{\parallel}/P_{\parallel} = \tan \delta_{\parallel} \qquad Q_{\perp}/P_{\perp} = \tan \delta_{\perp} \qquad (1)$$

The subscripts in eq 1 denote the vertical ($\parallel$) and horizontal ($\perp$) components of the emission, and the δ's are the phase delays with respect to the excitation.

Following the procedure used for the correction of the linear polarization of the fluorescence due to window birefringency (Paladini & Weber, 1981), we obtain

$$p_{\parallel} = P_{\parallel}(1 - \alpha) + P_{\perp}\alpha \qquad p_{\perp} = P_{\perp}(1 - \alpha) + P_{\parallel}\alpha$$
$$q_{\parallel} = Q_{\parallel}(1 - \alpha) + Q_{\perp}\alpha \qquad q_{\perp} = Q_{\perp}(1 - \alpha) + Q_{\parallel}\alpha \qquad (2)$$

where p and q refer to the emerging light and P and Q to the incident light. We define

$$\cot \Delta_{obsd} = (p_\| p_\perp + q_\| q_\perp)/(p_\| q_\perp - p_\perp q_\|)$$

and

$$\cot \Delta_0 = (P_\| P_\perp + Q_\| Q_\perp)/(P_\| Q_\perp - P_\perp Q_\|) \qquad (3)$$

From these definitions and eq 2

$$\cot \Delta_{obsd} = [(\cot \Delta_0)/(1 - 2\alpha)][1 + C\alpha(1 - \alpha)] \qquad (4)$$

where

$$C = [(P_\| - P_\perp)^2 + (Q_\| - Q_\perp)^2]/(P_\| P_\perp + Q_\| Q_\perp) \qquad (5)$$

Figure 9 shows the value of C for a limiting anisotropy of 0.4 as a function of the parameters $\omega\tau$ (circular frequency times lifetime) and $6R\tau$(6 times rotational rate times lifetime). Only exceptionally does the value of C approach or exceed unity, remaining in general well below it. Moreover, C de-creases monotonically with the limiting anisotropy. As $\alpha(1 - \alpha)$ is less than 0.1, a satisfactory correction is obtained by taking

$$\tan \Delta_0 = \tan \Delta_{obsd}/(1 - 2\alpha) \qquad (6)$$

The experimental procedure for the determination of α is given by Paladini & Weber (1981) and by P. L.-G. Chong and G. Weber (unpublished results).

References

Paladini, A. A. (1980) Ph.D. Thesis, University of Illinois, Urbana, IL.
Paladini, A. A., & Weber, G. (1981) *Rev. Sci. Instrum. 52* (*3*), 419–427.
Weber, G. (1977) *J. Chem. Phys. 66*, 4081–4091.

Intervesicular Phospholipid Transfer. A Free-Flow Electrophoresis Study[†]

Marcel De Cuyper,* Marcel Joniau, and Hugo Dangreau

ABSTRACT: Using the free-flow electrophoresis technique, the spontaneous transfer or exchange of phospholipid molecules between differently charged phospholipid vesicles has been examined. The basic experiment concerns the transfer phenomena occurring in a mixture of equal amounts of dimyristoylphosphatidylcholine (DMPC)–dimyristoylphosphatidylglycerol (DMPG) (molar ratio 9:1) vesicles and DMPC vesicles above their gel-to-liquid-crystal phase transition. At 33 °C in 5 mM 4-morpholineethanesulfonic acid buffer (pH 6.0)–10 mM potassium chloride, the two peaks in the electrophoretograms approach each other according to a first-order reaction rate, indicating that DMPG moves from one vesicle population ("donor") to the other ("acceptor"). The half-time of the overall kinetic process (41 min) is independent of total lipid concentration but increases considerably with increasing ionic strength. These findings are consistent with a transfer of phospholipid through the aqueous phase. The transfer properties of the phosphatidylglycerol molecule are strongly affected by its fatty acyl side chain composition. As compared with DMPG, the transfer of dioleoyl-phosphatidylglycerol occurs much faster, whereas in the case of dipalmitoylphosphatidylglycerol (DPPG) immobile electrophoretograms are found. Transfer of DMPG also depends on the relative fluidity of the donor membranes. Substituting DMPC by dioleoylphosphatidylcholine (DOPC) in the donor vesicles doubles the half-time for DMPG transfer, whereas changing DMPC in the neutral acceptor vesicles by DOPC has no effect. A different approach has been used to examine separately the individual transfer rates of DMPG and DMPC. Use was made of DMPC–DPPG (molar ratio 9:1) and DMPC vesicles, a mixture of which produces immobile electrophoretograms. Either the neutral or anionic vesicle population was labeled with either [³H]DMPC or [³H]DMPG. In these experiments, the half-times for transfer are calculated from the changes in radioactivity associated with the neutral or the anionic vesicle population. It appears that the transfer behavior of DMPG—in contrast to that of DMPC—is strongly affected by the charge properties of the membranes. Indirectly, we also deduce that flip-flop movements occur at a faster rate than intervesicular phospholipid transfer.

Spontaneous phospholipid transfer or exchange has been established by using a wide variety of techniques (Dawidowicz & Rothman, 1976; De Kruijff & Van Zoelen, 1978; McLean & Phillips, 1981; Nichols & Pagano, 1981; Roseman & Thompson, 1980). Comparing the different results, however, remains difficult. Indeed, evidence has been presented in support of two fundamentally different mechanisms: one involving transfer upon collision (Martin & MacDonald, 1976) and the other involving transfer from the monomeric (or micellar) pool of phospholipid, which is in equilibrium with the bilayer phase (McLean & Phillips, 1981; Roseman & Thompson, 1980). Also, in studies of phospholipid transfer phenomena, attention has been focused mainly on the influence of the fatty acyl chain length of the molecules, thereby neglecting the influence of double bonds and the role played by the polar head-group type. For instance Duckwitz-Peterlein et al. (1977) found that the shorter *trans*-9-hexadecenoate-containing phospholipid molecules move more rapidly than *trans*-9-octadecanoate-containing ones. Although these authors mention that their vesicle types contain about 20% acidic phospholipids, the individual contribution of these to the overall process was not checked.

Intervesicular interactions between differently charged membrane structures have been approached by using the ion-exchange chromatography technique with dicetyl phosphate or phosphatidic acid as an immobile anionic membrane component of the donor and/or acceptor vesicle population (De Kruijff & Van Zoelen, 1978; McLean & Phillips, 1981; van den Besselaar et al., 1975). Direct measurements of spontaneous phospholipid transfer of negatively charged phospholipids by this method have not been reported. In